Desalination and Water Treatment
www.deswater.com
doi: 10.5004/dwt.2019.23795

149 (2019) 98–104
May

Control strategy for nitrate reduction by sulfate green rust: the key role of copper and aluminum

Yongsheng Lu, Yangyi He, Jizhi Zhou, Xueer Huang, Lu Xu, Zulong Wu, Yunfeng Xu*, Guangren Qian

School of Environmental and Chemical Engineering, Shanghai University, No. 99 Shangda Rd., Shanghai 200444, China, Tel. +86 21 66137771/+86 21 66137745; Fax: +86 21 66137756; email: yfxu@shu.edu.cn (Y. Xu), Tel. +86 21 66137748; email: luys7174@shu.edu.cn (Y. Lu), Tel. +86 21 66137761; email: juice716@163.com (Y. He), Tel. +86 21 66137746; email: jizhi.zhou@t.shu.edu.cn (J. Zhou), Tel. +86 21 66137761; emails: 1012163861@qq.com (X. Huang), xulu_deer@163.com (L. Xu), davidwzl@126.com (Z. Wu), Tel. +86 21 66137758; email: grqian@shu.edu.cn (G. Qian)

Received 19 August 2018; Accepted 12 January 2019

ABSTRACT

The nitrate reduction velocity by sulfate green rust via the intervention of copper and aluminum (GR–SO_4^{2-}(Cu–Al)) can be controlled. The experiment was performed using a batch of reactor systems. First, the results indicated that the addition of Cu(II) to GR–SO_4^{2-} improved the nitrate reduction rate by a maximum of 3.5 times compared with GR–SO_4^{2}. Second, Al substitution enabled a gradual transformation from nitrate to nitrite instead of a rapid transformation from nitrate to ammonium. When nitrite accumulated in the solution, it might generate other possible intermediate products, such as NO, N_2O, and N_2 formation. The results indicated that a maximum total nitrogen removal efficiency of nearly 25% was obtained at pH = 9 using GR–SO_4^{2-} doping with 3% Cu^{2+} and Al^{3+}/trivalent metal (M^{3+}) = 20%. And the results of experiments were compared by conducting a first-order kinetics. Additionally, the results obtained using X-ray diffraction indicated that magnetite and goethite were produced in the process of nitrate and GR–SO_4^{2-}(Cu–Al).

Keywords: Green rust; Nitrate reduction; Copper; Aluminum; TN removal

1. Introduction

The presence of water source contamination with nitrogen-containing compounds has become a serious concern due to intensive agricultural activities [1] and industrial and domestic disposal [2]. High nitrate (NO_3^-) concentrations in water sources cause a potential risk to the environment and public health [3,4]. Conventionally, nitrate removal proceeds via biological denitrification [5,6] and physicochemical technologies [7]. To remove nitrate from water, chemical reduction methods have gained the interest of researchers because they can degrade nitrate faster than biological methods and are more cost effective than physicochemical methods [8].

Previous studies have investigated nitrate reduction by zerovalent iron (Fe^0) [9] or other iron-bearing minerals [10,11]. However, in the nitrate reduction process with Fe^0, ammonium is the only product, and the reaction is significantly influenced by the solution pH [12]. In addition, structural Fe^{2+} is more reactive than dissolved Fe^{2+} [13]. Among these Fe(II)-bearing minerals, green rusts (GR) comprise layered Fe(II)–Fe(III) hydroxide that is composed of alternating positively charged layers and negatively charged interlayers that contain water molecules and anion [14].

---

* Corresponding author.

They have been investigated for several years as the chemical reductant for nitrate reduction [15]. Hansen et al. [16] have analyzed nitrate reduction by GR. Due to the low rate of the reaction for GR with nitrate, Choi et al. [11] have enhanced the nitrate reduction rate of nitrate by GR with the addition of nine different trace metals. Nitrate was converted to ammonium completely in a previous study, although GR can rapidly reduce nitrate. Nitrogen remained in the solution as ammonium, which did not achieve the goal of reducing total nitrogen (TN). In our previous study [17], we reduced TN and NO_2^- with GR by adjusting the initial E_h, which controlled the generation of different reduction products (N_2O, N_2 and NH_4^+) in the process. Vorlop et al. [18,19] demonstrated that supported bimetallic catalyst can reduce nitrate to harmless nitrogen gas. Consequently, GR modified by bimetal may improve nitrogen removal by controlling the reaction efficiency and selectivity.

In this study, two metals (copper and aluminum) were doped into sulfate green rust ($GR–SO_4^{2-}$).The rate and direction of reaction between nitrate and $GR–SO_4^{2-}$ via the intervention of copper and aluminum ($GR–SO_4^{2-}$(Cu–Al)) can be regulated. The effects of each metal and their amounts were investigated in a solution of 40 mg N L^{-1}. The oxidation-reduction potential (ORP) and pH have been investigated to achieve real-time control of nitrate removal [20]. The ORP and pH were monitored in real time. The most effective combinations were selected based on both the reaction rate constant and the removal of TN. The influence of GR substituted by two metals on the efficiency of nitrate reduction has not been reported.

Therefore, the objective of this study was to explore the relationship between removal efficiency of nitrate or TN and $GR–SO_4^{2-}$(Cu–Al). Meanwhile, it was investigated that ORP may underlie the improvement of the removal rate.

2. Materials and methods

2.1. Preparation of $GR–SO_4^{2-}$ doped with Cu(II) and Al(III)

For this study, $GR–SO_4^{2-}$ was synthesized by a co-precipitation method with bubbling helium gas (He) [21,22]. A mixture of $FeSO_4·7H_2O$ (0.02 mol Fe^{2+}), $Fe_2(SO_4)_3·5H_2O$, and $Al_2(SO_4)_3·18H_2O$ [$m(Fe^{3+}) + n(Al^{3+})$, $m + n = 0.01$ mol] was dissolved in 100 mL of double-distilled water that was adequately purged with He in a 500-mL flask with the ratio of $n(Al^{3+})/n(M^{3+})$ = 0%~40%. The addition of Cu(II) with the ratio of $n(Cu^{2+})/n(M)$ = 0%~5% was achieved by contacting the suspension with $CuSO_4·5H_2O$ using fast magnetic stirring. Then, NaOH solution (1 M) was continuously added to the solution under the condition of magnetic stirring until the pH of the suspension was 7. The samples were aged for 20 h at an approximate temperature of 25°C, which dried in a vacuum freeze drier after being filtered through a 0.45-μm filter membrane. All chemicals employed in this study were purchased from Sinopharm Chemical Reagents (Shanghai, China) and were of analytical grade.

2.2. Experiments for nitrate removal

A batch of experimental instruments were composed of a 500-mL boiling flask-4-neck, pH electrode, ORP electrode, and thick butyl rubber stopper accompanied by magnetic stirring. The reaction began by spiking 100 mL of sodium nitrate solution with initial NO_3^-–N concentrations of 40 mg L^{-1} (C_0) into a $GR–SO_4^{2-}$ suspension. In the course of the reaction, the values of the ORP and pH were also monitored. At regular time intervals, the samples were collected and filtered using a 0.22 μm filter membrane. The nitrate concentration of NO_3^-–N (C_t) at sampling time was determined. The removal efficiency was calculated as removal efficiency (%) = $(C_0 - C_t)/C_0 \times 100$.

2.3. Analysis

X-ray diffractometer (XRD) patterns of the samples were recorded on a Rigaku D/max RBX XRD with Cu-Kα radiation ($\lambda = 0.154$ nm). The scanning rate was 8°min^{-1} in the 2θ range of 5°–80°.

Continuous monitoring of pH and E_h were detected using a pH electrode (PHS-3C) and an ORP electrode (501 ORP, Shanghai INESA Science Instrument CO, LTD) [23]. NO_2^-, NO_3^-, NH_4^+, and TN in the sample supernatant were measured by spectrophotometry (UNICO, UV-2100) [24].

3. Results and discussion

3.1. Characterization of GR

In this study, a co-precipitation method was adopted to prepare $GR–SO_4^{2-}$, $GR–SO_4^{2-}$(Cu), and $GR–SO_4^{2-}$(Cu–Al). The dried samples were dark green. The wide-angle XRD patterns of $GR–SO_4^{2-}$ exhibited the main diffraction plane at (001), (002), and (003) (Fig. 1(a)) and were similar to the previously reported data for $GR–SO_4^{2-}$ [21]. The XRD patterns of the samples with different Al^{3+}/M^{3+} ratios are also observed in the same peaks (Fig. 1(c)), which represented the (001), (002), and (003) crystal plane diffraction angle as a multiple relation. The weak reflection (Fig. 1(b)) at 21.2° and 33.2° (2θ) is assigned to the oxidation products of GR and goethite. No significant shift of the (001) lines is indicated in Fig. 1.

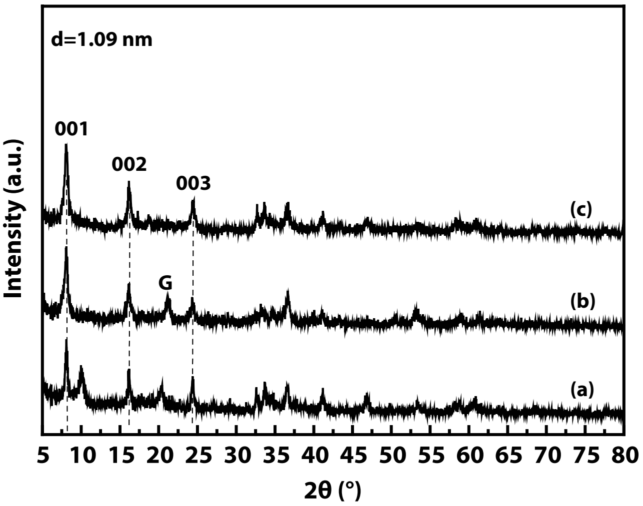

Fig. 1. XRD patterns of GR samples. (a) $GR–SO_4^{2-}$ alone, (b) $GR–SO_4^{2-}$ added with Cu(II), Cu^{2+}/M = 3%, and (c) $GR–SO_4^{2-}$ added with Cu(II) and Al(III), Al^{3+}/M^{3+} = 20%, goethite (α–FeOOH).

Therefore, the presence of Cu^{2+} and Al^{3+} did not destroy the structure of the interlayer distance along the (001) direction (d = 1.09 nm) [22], which was primarily governed by the nature of the intercalated anion SO_4^{2-}. All samples belonged to the "GR-type layered doubled hydroxides" [25].

Inductively coupled plasma-atomic emission spectrometry was introduced to detect the metallic elements, such as Cu, Al, and Fe, in the filtrate. The results indicated that Cu and Al were below the detection limit, which indicated that Cu^{2+} and Al^{3+} had been successfully converted to the solid phase in the GR–SO_4^{2-} samples. According to the solubility product (Ksp) of $Fe(OH)_3$, $Al(OH)_3$, $Cu(OH)_2$ and $Fe(OH)_2$, the co-adsorption of soluble Al(III), Cu(II), and Fe(II) onto the initially precipitated ferric oxyhydroxides may serve a primary role during the formation of GR–SO_4^{2-}(Cu–Al).

3.2. Comparison of different types of GR–SO_4^{2-} on nitrate reduction

Fig. 2 indicates the results of nitrate reduction by GR–SO_4^{2-}, GR–SO_4^{2-}(Cu), and GR–SO_4^{2-}(Cu–Al) with a pH value of 9.0 ± 0.2 at room temperature. In Fig. 2(a), no significant nitrate loss occurred with GR–SO_4^{2-} during 150 min, and ammonium increases as the final product of nitrate reduction without any by-products being detected. The average rate of nitrate reduction was 2.67 mg L^{-1} h^{-1}. Hansen et al. [26] investigated nitrate reduction by GR–SO_4^{2-}; the reaction rate of nitrate reduced with GR–SO_4^{2-} was very slow, and the average rate of nitrate reduction was 0.32 mg L^{-1} h^{-1}.

As shown in Fig. 2(b), the nitrate reduced by GR–SO_4^{2-} modified by Cu. The average rate of nitrate reduction by GR–SO_4^{2-}(Cu) was 9.35 mg L^{-1} h^{-1}, which was enhanced by a factor of 3.5 compared with GR–SO_4. Previous studies have shown that the addition of Cu(II) to GR–SO_4^{2-} increased the rate of carbon tetrachloride reduction [27]. These results demonstrated that the addition of Cu to GR enhanced the reaction rate. The initial concentration of nitrate rapidly decreased within 30 min but nitrite simultaneously increased. In the subsequent hour, nitrite slowly decreased. Ammonium was the main product, and TN did not distinctly reduce. These results are consistent with the findings of Choi et al. [28], who suggested that Cu enhances the rate of reduction and all nitrates were transformed to ammonium. In addition, Hansen et al. have confirmed that sulfate GR materials did not absorb nitrate or nitrite or ammonium [29].

Fig. 2(c) shows the results of the nitrate reduction by GR–SO_4^{2-}(Cu–Al). These results demonstrated that Al substitution in GR–SO_4^{2-}(Cu) yielded the same faster rate of nitrate removal as GR–SO_4^{2-}(Cu), whereas modified GR had a four times faster reaction rate than GR. Nitrite was increased in reaction processes for 90 min. Nitrite gradually disappeared in the reaction with GR–SO_4^{2-}(Cu–Al) system. The concentration of ammonium with GR–SO_4^{2-}(Cu–Al) was lower than the concentration of ammonium with GR–SO_4^{2-}(Cu).

The decreased percentages of TN were 10.8% and 23.4% in the reaction with GR–SO_4^{2-}(Cu) and GR–SO_4^{2-}(Cu–Al), respectively. In the process of reaction, no ammonia gas

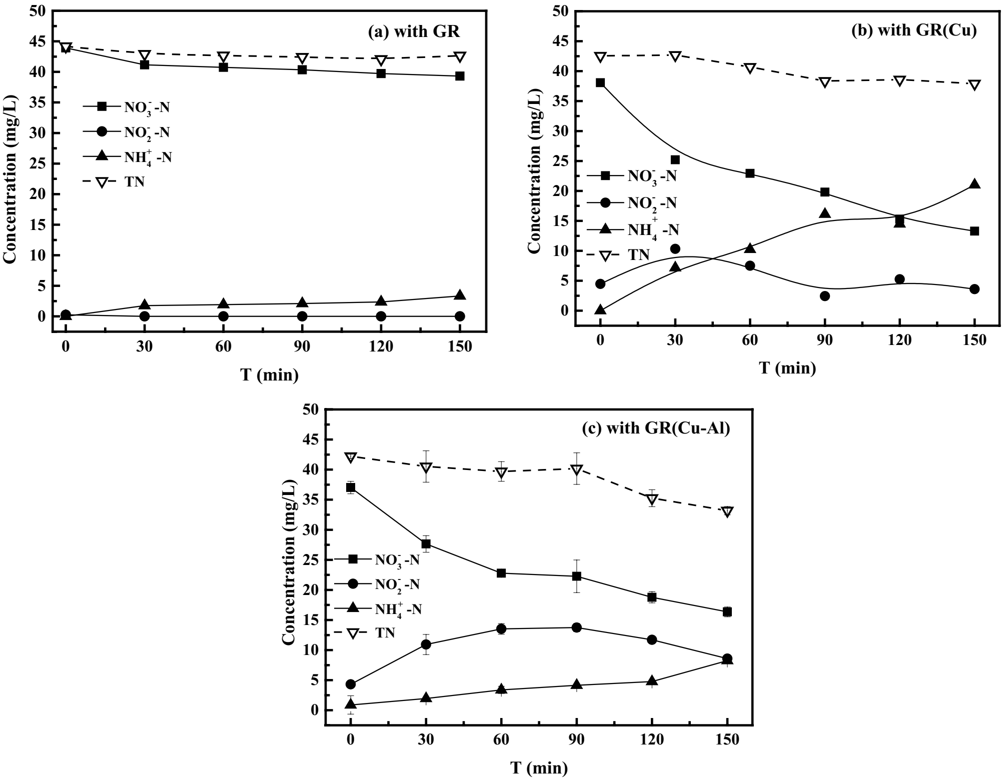

Fig. 2. Various curves with time of nitrate, nitrite, and ammonium during a batch test of nitrate reduction by (a) GR–SO_4^{2-}, (b) GR–SO_4^{2-}(Cu), and (c) GR–SO_4^{2-}(Cu–Al). The initial nitrate concentration was approximately 40 mg N L^{-1}. The Cu(II) addition was 3% of all metals. The Al^{3+}/M^{3+} ratio was 20%.

was detected. The results indicated that GR–SO_4^{2-}(Cu–Al) exhibited higher efficiency than GR–SO_4^{2-}(Cu) to reduce TN.

3.3. Rate controlling for nitrate reduction with Cu(II) dosage

Fig. 3 shows the effect of different Cu(II) addition on nitrate reduction by GR–SO_4^{2-}(Cu) at pH 9.0 ± 0.2. The effect on nitrate reduction of the addition of Cu(II) to GR–SO_4^{2-} was investigated for the range of 0%–5% for all metals (Cu^{2+}/M). With an increase in Cu(II) addition, a distinct increase in the nitrate removal efficiency was observed. In addition, 3% addition of Cu(II) gained the highest removal efficiency of 80%. However, 5% addition of Cu(II) decreased the reduction efficiency. An appropriate addition of Cu(II) accelerated the rate of nitrate reduction by Fe(II) sorbed onto ferric iron oxy-hydroxides [30]. Similar results were obtained while enhancing dechlorination of the chlorinated hydrocarbons by GR–Cl^- (Cu) [31]. These studies depicted that Cu(II) added to GR was reduced to a zerovalent form of Cu, which catalytically served an important role in electron transfer from Fe(II) on the GR surface to the contaminant. A possible equation is Eq. (1).

$$Fe_4^{II}Fe_2^{III}\left(OH\right)_{12}SO_4 + 2Cu^{2+} \rightarrow 6FeOOH + 2Cu^0 + SO_4^{2-} + 6H^+ \quad (1)$$

However, the nitrate removal efficiency decreased with the addition of 5% Cu(II). Previous studies have reported the effect of Cu(II) on the kinetics of nitrate reduction by GR–F^-. A large amount of Cu(II) may consume too much Fe(II), which caused an insufficient amount of Fe(II) to be employed for rapid nitrate reduction [32].

3.4. Direction control for nitrate reduction with Al substitution

The Al^{3+}/M^{3+} ratio in GR–SO_4^{2-}(Cu–Al) can influence the direction of nitrate removal. The addition of Cu(II) in GR–SO_4^{2-}(Cu–Al) was 3% of all metals in the following experiments: Cu(II) was added to improve the velocity of reaction due to the low reactivity of nitrate reduction by GR–SO_4^{2-}. As shown in Fig. 4, the substitution of Al ($r = n(Al^{3+})/n(M^{3+})$ = 0%, 10%, 20%, and 30%) was used to evaluate the removal of the TN. The influence of the Al^{3+}/M^{3+} ratio on TN removal exhibited a fluctuation. When the Al^{3+}/M^{3+} ratio was 20%, the TN achieved the maximal removal efficiency of 25%. However, nitrogen-containing products remained in the water with the maximum capacity of Al.

During nitrate reduction by GR–SO_4^{2-}(Cu–Al), nitrate was not adsorbed onto the GR surface, and it was converted to nitrite. Al substitution of Fe(III) in GR can effectively reduce the reactivity of Fe(II) in GR and decelerate the rate of transformation of NO_3^- to NH_4^+. Figs. 2(c) and 5(a) both show that nitrite accumulated for a relatively long time in the solution, which provided the possibility of the transformation from nitrite to other intermediates. Liou et al. [33] proposed that nitrite accumulation occurred in the reaction process of relatively high N_2 selectivity during nitrate reduction by iron-deposited bimetals. Elemental analysis was employed to characterize the existence of nitrogen element in solid, whereas no nitrogen was detected. According to the nitrogen mass balance, the decrease of TN may be reduced to other types of gaseous nitrogen species, such as NO, N_2O, or N_2. Al substituted in GR–SO_4^{2-} [34] controlled the reaction pathway and effectively reduced the TN.

The wide-angle XRD analyses of GR–SO_4^{2-}(Cu–Al) products indicated that magnetite and goethite were the main products of the reaction of GR–SO_4^{2-}(Cu–Al) with nitrate (Fig. 5(b)). However, weak diffraction peaks are observed at 8.1°, 16.1°, and 24.3° (2θ), which indicated that part of GR–SO_4^{2-}(Cu–Al) persisted in the reaction. Previous studies have documented that Al adsorption and substitution is helpful for protecting ferrihydrite, which may impede lepidocrocite formation and magnetite nucleation [35]. The excessive content of Al reduced the reduction efficiency.

3.5. The kinetic analysis of nitrate reduction

The removal of nitrate by GR was deemed to be a first-order kinetics or pseudo-first-order kinetics. According

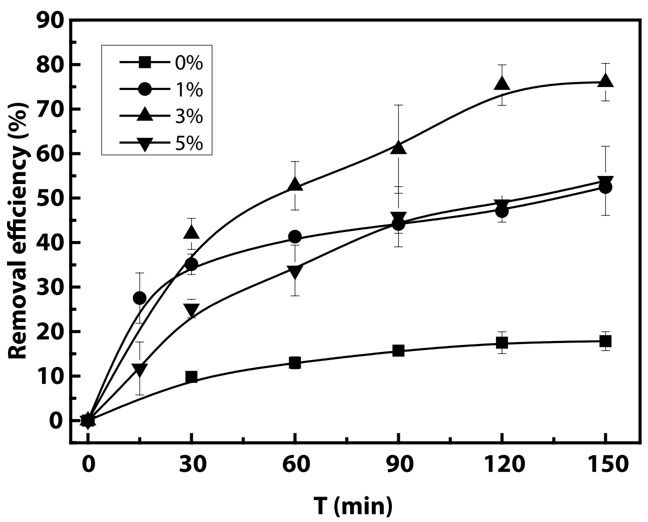

Fig. 3. Effect of different addition of Cu(II) dosages to GR on nitrate removal.

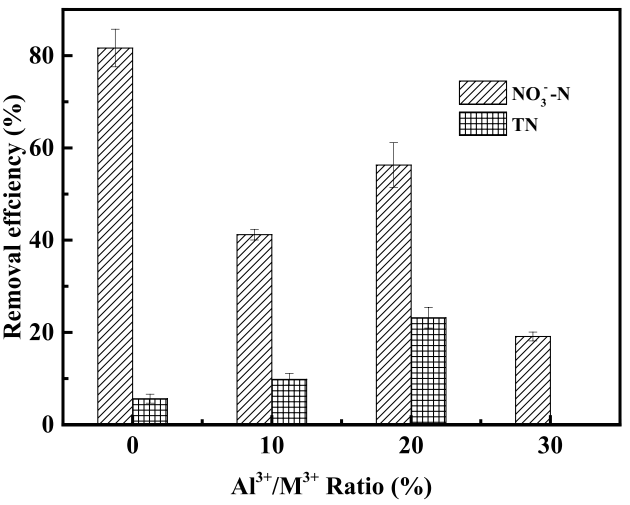

Fig. 4. Nitrate and total nitrogen removal efficiency in aqueous solution with the dependence of different amounts of aluminum. The Cu(II) addition was 3% of all metals.

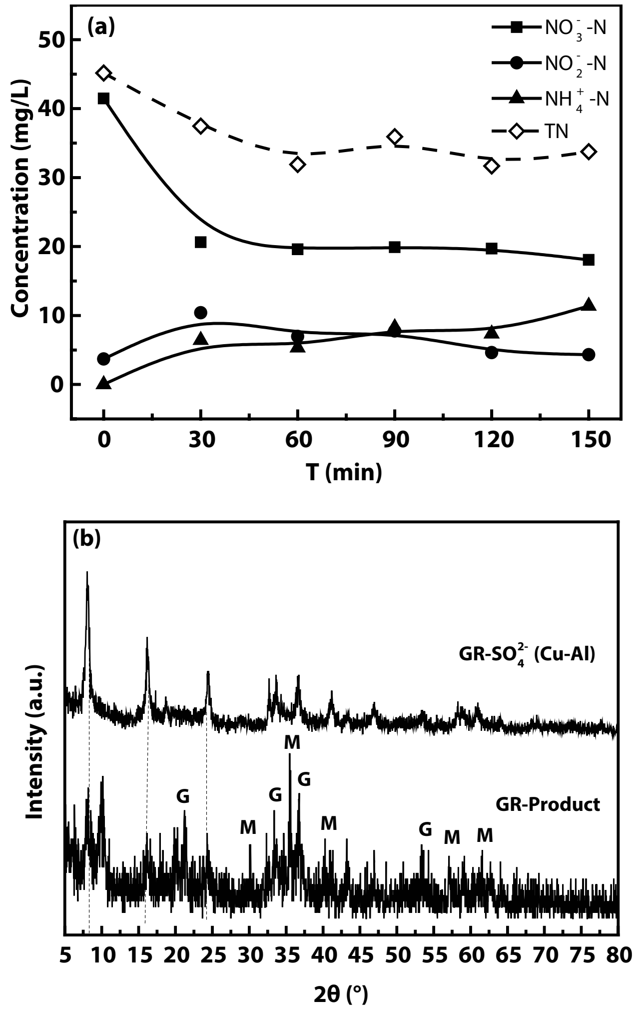

Fig. 5. Nitrogen mass balance during the reaction of GR–SO_4^{2-} (Cu–Al) with nitrate (a) and solid-phase transformation (b).

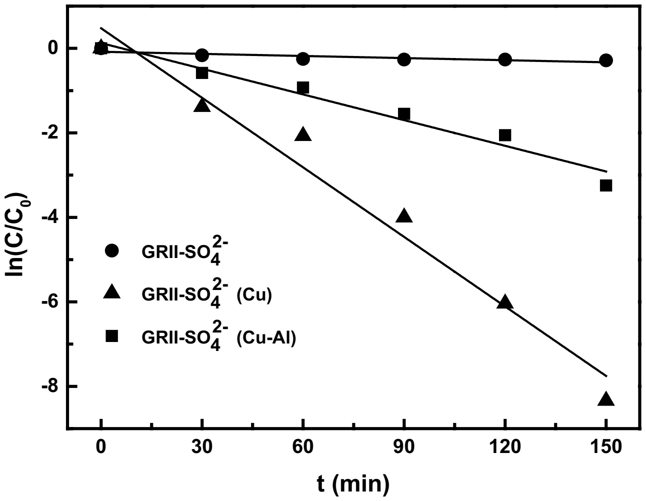

Fig. 6. First-order kinetic fitting of nitrate react with GR–SO_4^{2-}, GR–SO_4^{2-}[31], and GR–SO_4^{2-}(Cu–Al).

Table 1
The apparent rate constant of nitrate react with GR–SO_4^{2-}, GR–SO_4^{2-}(Cu), and GR–SO_4^{2-}(Cu–Al)

GRs	k_{obs} (min^{-1})	R^2
GR–SO_4^{2-}	0.0016	0.6621
GR–SO_4^{2-}(Cu)	0.0549	0.9644
GR–SO_4^{2-}(Cu–Al)	0.0203	0.9541

to the fitting formula, Eq. (2), the first-order kinetics of the reaction of GR–SO_4^{2-}, GR–SO_4^{2-} [34], and GR–SO_4^{2-}(Cu–Al) with nitrate were obtained.

$$k = \frac{1}{t}\ln\left(\frac{C_0}{C}\right) \tag{2}$$

where k is reaction rate constant, t is the reaction time, C_0 is the initial concentration of nitrate, and C is the concentration at moment of t. In the case of pH value at 9 and 40 mg L^{-1} of initial nitrate concentration and other parameter stayed the same, the ln(C_0/C) – t fitting curves of concentration of nitrate for the reaction of various GRs are exhibited in Fig. 6.

The apparent rate constants k_{obs} in the processes of the removal of nitrate by GRs were calculated from Fig. 6 and are listed in the Table 1. As shown in the table, the linear relationship of ln(C_0/C) – t curves was obvious corresponding to the reaction of nitrate with GR–SO_4^{2-}(Cu) and GR–SO_4^{2-}(Cu–Al). Meanwhile, the k_{obs} of GR–SO_4^{2-}, GR–SO_4^{2-}(Cu), and GR–SO_4^{2-}(Cu–Al) was 0.0016, 0.0549, and 0.0203 min^{-1}, respectively. These indicated that the reaction rate of GR–SO_4^{2-}(Cu) with nitrate is nearly 40 times higher than GR–SO_4^{2-}, and the removal efficiency of nitrate by GR–SO_4^{2-} (Cu–Al) is 15 times than GR–SO_4^{2-}.

The doping of Cu(II) greatly increased the reactivity of GR to nitrate. The substitution of Al(III) for Fe(III) reduced the reducibility of GR; however, because of the presence of Cu(II), the removal rate was still much higher than GR–SO_4^{2-} without Cu and Al.

3.6. Reduction product profiles for different initial E_h

To explore the relationship between the reduction products and E_h, the trends of E_h and reaction products are listed in Table 2. Since the reactions were performed in an anaerobic condition, the value of dissolved oxygen was very low, which had minimal impact on the E_h. In a typical experiment at the initial pH 9, the fluctuation range of the E_h varied, which produced an excellent rate and efficiency for the chemical reduction of nitrate by various GR.

A total of 84.81% of the nitrate remained in the system with GR–SO_4^{2-}, whereas E_h increased from –626 to –595 mV. The addition of Cu significantly changed E_h, 65.27% of NO_3^-–N was reduced by GR–SO_4^{2-}(Cu) when the initial E_h ranged from –515 to –442 mV. The E_h value ranged from –515 to –407 mV with an increase in the Al content. The majority

Table 2
Relationship between the ORP during nitrate reduction and nitrogen content with controlling the pH value at approximately 9

Material	E_h (mV)	Concentration (N%)			Ng
		NO_3^-–N	NO_2^-–N	NH_4^+–N	
GR alone	–626 to –595	84.81	ND	15.19	0
GR(Cu–Al), Al/M^{3+} = 0%	–515 to –442	34.73	6.52	59.56	0
GR(Cu–Al), Al/M^{3+} = 10%	–493 to –436	30.98	12.73	50.67	5.62
GR(Cu–Al), Al/M^{3+} = 20%	–488 to –409	30.14	0.97	43.02	25.87
GR(Cu–Al), Al/M^{3+} = 30%	–425 to –407	80.31	12.71	6.46	0.52

of the nitrate was reduced, and nitrite was detected with Al addition to GR–SO_4^{2-}(Cu). Nitrite gradually decreased with the addition of 20% Al, and approximately 25% TN was reduced. These results indicated that Al substitution slightly diminished the reductive environment of the solution, which was suitable for the transformation from nitrate to intermediate products, such as nitrite. With a very strong reducing capacity (E_h = –600 mV) without Al, nitrate rapidly converted to ammonia without generating any intermediate products.

The majority of the reports have indicated NH_4^+ as the end product of nitrate reduction by GR. NO_2^- was not observed in the solution, whereas all NO_3^- transformed to NH_4^+ [29]. In this study, Al substitution of Fe(III) in GR–SO_4^{2-} promoted the formation of nitrite. Nitrite accumulated in the solution for a relatively long time and then disappeared with a decrease in TN. Previous studies have shown that strong reducing conditions (low ORP) favored the formation of ammonia, whereas gaseous nitrogen (NO, N_2O, and N_2) formation was favored in moderate or low reducing conditions (high ORP) [36]. Furthermore, the reduction of nitrite with GR was controlled by ORP used of different pH values [18]. Al substitution into GR–SO_4^{2-}(Cu) affected the initial E_h, which favored the yield of Ng and the removal efficiency of NO_2^-. This finding indicated that part of the nitrate was converted to the intermediate products, such as NO, N_2O, or N_2 gas via nitrite and escaped from the solution in the experiments. The doping of metals (Cu^{2+} and Al^{3+}) into GR–SO_4^{2-} can significantly enhance the reaction rates and control the reduction products, which involves changes in the ORP; this finding is consistent with the observation by Wu et al. [37].

4. Conclusions

In this study, the GR–SO_4^{2-}(Cu–Al) was synthesized by a co-precipitation method that was employed to reduce nitrate from solution. The addition of Cu to GR–SO_4^{2-} can enhance the reactivity of Fe(II) in GR–SO_4^{2-} and effectively improve the reaction rate. Al substitution of Fe(III) in GR–SO_4^{2-} can adjust the products and efficiency. A maximum TN removal of nearly 25% was obtained at pH = 9 using GR–SO_4^{2-} doping with 3% Cu, Al^{3+}/M^{3+} = 20%. The decrease of TN was observed in this study. However, nitrate was completely converted to ammonium in a previous study [11,27,29]. Nitrate was partly converted to nitrite rather than rapidly converted to ammonium, which enhanced other possible intermediate products, such as NO, N_2O, and N_2 formation. The loss of nitrogen is likely attributed to the emission of gaseous nitrogen species.

Acknowledgements

This work was financially supported by the National Nature Science Foundation of China (No. 41877187) and Program for Innovative Research Team in University (No. IRT13078).

References

[1] D. Tilman, K.G. Cassman, P.A. Matson, R. Naylor, S. Polasky, Agricultural sustainability and intensive production practices, Nature, 418 (2002) 671–677.

[2] F.T. Wakida, D.N. Lerner, Non-agricultural sources of groundwater nitrate: a review and case study, Water Res., 39 (2005) 3–16.

[3] L.J. Puckett, A.J. Tesoriero, N.M. Dubrovsky, Nitrogen contamination of surficial aquifers – a growing legacy, Environ. Sci. Technol., 45 (2011) 839–844.

[4] M. Sadeq, C.L. Moe, B. Attarassi, I. Cherkaoui, R. Elaouad, L. Idrissi, Drinking water nitrate and prevalence of methemoglobinemia among infants and children aged 1–7 years in Moroccan areas, Int. J. Hyg. Environ. Health, 211 (2008) 546–54.

[5] S.P. Burghate, D.N.W. Ingole, Biological water denitrification – a review, J. Environ. Sci. Comp. Sci. Eng. Technol., 3 (2014) 9–28.

[6] P. Cyplik, R. Marecik, A. Piotrowska-Cyplik, A. Olejnik, A. Drozdzynska, L. Chrzanowski, Biological denitrification of high nitrate processing wastewaters from explosives production plant, Water Air Soil Pollut., 223 (2012) 1791–1800.

[7] K.R. Reddy, T. Xie, S. Dastgheibi, Nutrient removal from urban stormwater by different filter materials, Water Air Soil Pollut., 225 (2014) 1778–1791.

[8] G.K. Luk, W.C. Au-Yeung, Experimental investigation on the chemical reduction of nitrate from groundwater, Adv. Environ. Res., 6 (2002) 441–453.

[9] P. Westerhoff, J. James, Nitrate removal in zero-valent iron packed columns, Water Res., 37 (2003) 1818–1830.

[10]] M. Etique, A. Zegeye, B. Gregoire, C. Carteret, C. Ruby, Nitrate reduction by mixed iron(II-III) hydroxycarbonate green rust in the presence of phosphate anions: the key parameters influencing the ammonium selectivity, Water Res., 62 (2014) 29–39.

[11] J. Choi, B. Batchelor, C. Won, J. Chung, Nitrate reduction by green rusts modified with trace metals, Chemosphere, 86 (2012) 860–865.

[12] S.H. Choe, H.M. Liljestrand, J. Khim, Nitrate reduction by zero-valent iron under different pH regimes, Appl. Geochem., 19 (2004) 335–342.

[13] Y.L. Tai, B.A. Dempsey, Nitrite reduction with hydrous ferric oxide and Fe(II): stoichiometry, rate, and mechanism, Water Res., 43 (2009) 546–552.

[14] G. Ona-Nguema, M. Abdelmoula, F. Jorand, O. Benali, A. Gehin, J.C. Block, J.M.R. Genin, Iron(II,III) hydroxycarbonate green rust formation and stabilization from lepidocrocite bioreduction, Environ. Sci. Technol., 36 (2002) 16–20.

[15] M. Usman, J.M. Byrne, A. Chaudhary, S. Orsetti, K. Hanna, C. Ruby, Magnetite and green rust: synthesis, properties, and environmental applications of mixed-valent iron minerals, Chem. Rev., 118 (2018) 3251–3304.

[16] H.C.B. Hansen, S. Guldberg, M. Erbs, C.B. Koch, Kinetics of nitrate reduction by green rusts – effects of interlayer anion and Fe(II): Fe(III) ratio, Appl. Clay Sci., 18 (2001) 81–91.

[17] Y. Lu, X. Yang, Z. Wu, L. Xu, Y. Xu, G. Qian, A novel control strategy for N_2O formation by adjusting E_h in nitrite/Fe(II–III) carbonate green rust system, Chem. Eng. J., 304 (2016) 579–586.

[18] U. Prüsse, M. Hähnlein, J. Daum, K.D. Vorlop, Improving the catalytic nitrate reduction, Catal. Today, 55 (2000) 79–90.

[19] U. Prüsse, K.D. Vorlop, Supported bimetallic palladium catalysts for water-phase nitrate reduction, J. Mol. Catal. A-Chem, 173 (2001) 313–328.

[20] D. Gao, Y. Peng, B. Li, H. Liang, Shortcut nitrification-denitrification by real-time control strategies, Bioresour. Technol., 100 (2009) 2298–2300.

[21] A. Gehin, C. Ruby, M. Abdelmoula, O. Benali, J. Ghanbaja, P. Refait, J.M.R. Genin, Synthesis of Fe(II-III) hydroxysulphate green rust by coprecipitation, Solid State Sci., 4 (2002) 61–66.

[22] R. Aissa, C. Ruby, A. Gehin, M. Abdelmoula, J.M.R. Genin, Synthesis by coprecipitation of Al-substituted hydroxysulphate green rust, Hyperfine Interact., 156/157 (2004) 445–451.

[23] S. Wang, J. Yu, T. Wei, Y. Chi, L. Sun, Y. Peng, Applying real-time control for achieving nitrogen removal via nitrite in a lab-scale CAST system, Environ. Technol., 33 (2012) 1133–1140.

[24] APHA, AWWA, WEF, Standard Methods for the Examination of Water and Wastewater, 20th Ed., American Public Health Association, Washington, DC, 1998.

[25] C. Ruby, M. Abdelmoula, R. Aissa, G. Medjahdi, M. Brunelli, M. François, Aluminium substitution in iron(II–III)-layered double hydroxides: formation and cationic order, J. Solid State Chem., 181 (2008) 2285–2291.

[26] H.C.B. Hansen, C.B. Koch, H. Nancke-Krogh, O.K. Borggaard, J. Sorensen, Abiotic nitrate reduction to ammonium: key role of green rust, Environ. Sci. Technol., 30 (1996) 2053–2056.

[27] E.J. O'Loughlin, K.M. Kemner, D.R. Burris, Effects of Ag-I, Au-III, and Cu-II on the reductive dechlorination of carbon tetrachloride by green rust, Environ. Sci. Technol., 37 (2003) 2905–2912.

[28] J. Choi, B. Batchelor, Nitrate reduction by fluoride green rust modified with copper, Chemosphere, 70 (2008) 1108–1116.

[29] H.C.B. Hansen, C.B. Koch, Reduction of nitrate to ammonium by sulphate green rust: activation energy and reaction mechanism, Clay Miner., 24 (1998) 663–669.

[30] C.J. Ottley, W. Davison, W.M. Edmunds, Chemical catalysis of nitrate reduction by iron(II), Geochim. Cosmochim. Acta, 61 (1997) 1819–1828.

[31] R.A. Maithreepala, R.A. Doong, Enhanced dechlorination of chlorinated methanes and ethenes by chloride green rust in the presence of copper(II), Environ. Sci. Technol., 39 (2005) 4082–4090.

[32] L. Simon, J.M.R. Génin, P. Refait, Standard free enthalpy of formation of Fe(II)-Fe(III) hydroxysulphite green rust one and its oxidation into hydroxysulphate green rust two, Corros Sci., 39 (1997) 1673–1685.

[33] Y.H. Liou, C.J. Lin, S.C. Weng, H.H. Ou, S.L. Lo, Selective decomposition of aqueous nitrate into nitrogen using iron deposited bimetals, Environ. Sci. Technol., 43 (2009) 2482–2488.

[34] Z.-Z. Zhang, J.-J. Xu, Z.-J. Shi, Y.-H. Bai, Y.-F. Cheng, H.-Y. Hu, R.-C. Jin, Unraveling the impact of nanoscale zero-valent iron on the nitrogen removal performance and microbial community of anammox sludge, Bioresour. Technol., 243 (2017) 883–892.

[35] C.M. Hansel, D.R. Learman, C.J. Lentini, E.B. Ekstrom, Effect of adsorbed and substituted Al on Fe(II)-induced mineralization pathways of ferrihydrite, Geochim. Cosmochim. Acta, 75 (2011) 4653–4666.

[36] B.P. Dash, S. Chaudhari, Electrochemical denitrification of simulated ground water, Water Res., 39 (2005) 4065–4072.

[37] D.L. Wu, B.B. Shao, M.Y. Fu, C. Luo, Z.G. Liu, Denitrification of nitrite by ferrous hydroxy complex: effects on nitrous oxide and ammonium formation, Chem. Eng. J., 279 (2015) 149–155.